CHAPTER IV
RESULTS AND DISCUSSION

In this chapter, there are three experimental results to be discussed; the characteristics of W/O microemulsion solution, the sequential mechanisms of silica particle formation from TBOS, and the controlled the size distribution of silica particle using butanol. All experimental data are shown in Appendix A.

4.1 Characteristics of W/O Microemulsion Solution

In this study, W/O microemulsion system was used to synthesize silica particles from TBOS hydrolysis via ammonium based catalyst. The characteristics and physical-chemical properties of W/O microemulsion solution are depended on its system components. Therefore, the diagram of phase boundary can be described the fundamental properties of the colloid solution (i.e., solubilization of aqueous component). The dimension of W/O microemulsions was investigated by using dynamic light scattering (DLS).

4.1.1 Phase Diagram of DP6/Water/Heptane System

The W/O microemulsion solution containing of DP6, heptane, ammonium, and water was prepared at 22 ^{0}C. The particular compositions of each system component afford the single-phase W/O microemulsion (transparent solution). Figure 4.1 shows the boundary phase diagram of DP6/heptane/aqueous ammonia and DP6/heptane/aqueous ammonia/butanol systems. There are three curves that represent the solubility of aqueous ammonia in both systems. The phase boundary indicates the single-phase and

two-phase regions. For the single-phase region, which is below the curves for each system, water and aqueous ammonia are completely solubilized in W/O microemulsion solution. On the other hand, in the two-phase region, the excessive amount of water causes a second water-rich phase.

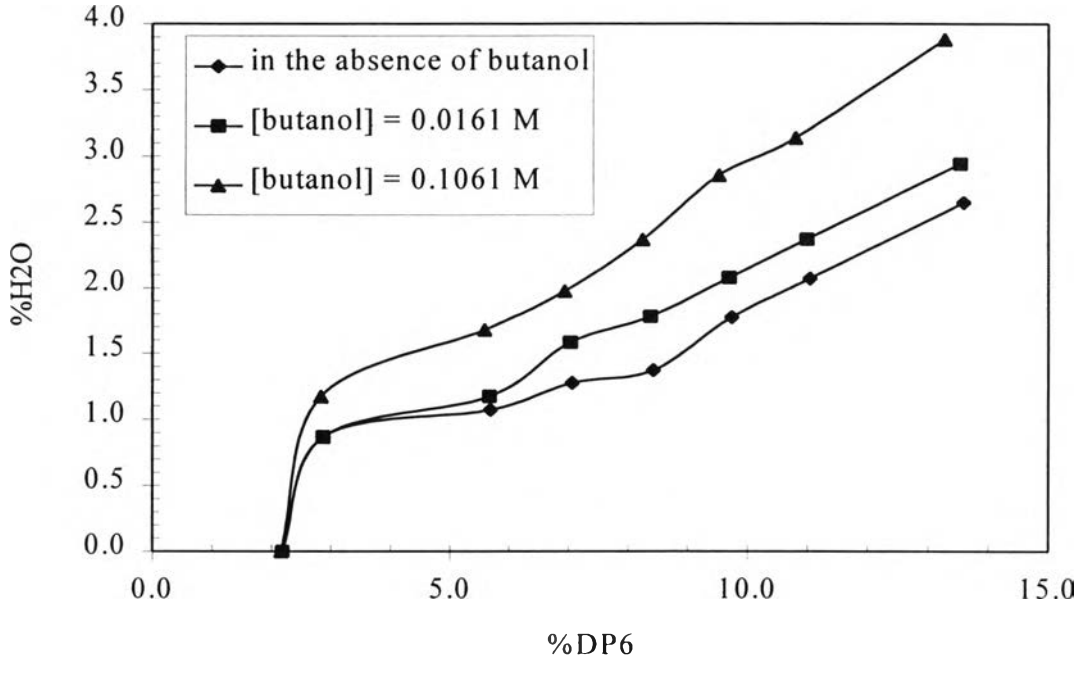

Figure 4.1 Phase diagrams of DP6/heptane/water systems in the presence and absence of butanol

For all of systems, aqueous ammonia could be clearly solubilized in W/O microemulsion solution, after adding the DP6 concentration until 2.02 %. Beyond this DP6 concentration, the solubilities of water and aqueous ammonia increased drastically, when the DP6 concentration was increased. Ammonia molecules and hydroxide ions may behave as lyotropic constituents; weakening the water-surfactant interaction or disrupting the hydrogen-bonding structure of pure water (Arrigada, 1991). The phase diagram also describes the solubilities of water and aqueous ammonia increase with increasing of butanol concentration. In this study, butanol was applied as a co-surfactant in the

microemulsion system. It results in creating hydrogen-bonding between hydroxyl group (-OH) of butanol and ethoxyl groups (-OE) of the surfactant molecule, leading to increasing the hardness of surfactant film (Esquena et al., 1997).

4.1.2 Effect of Butanol Concentration on Size of Micelle Droplets

In this experiment, the size of W/O microemulsion droplets were measured in terms of hydrodynamic diameter (D_h) by using dynamic light scattering (DLS). Figure 4.2 illustrates the effect of butanol concentration on hydrodynamic diameter. The specimen system used consisted of 0.9460 M of DP6, 0.1017 M of NH_3, and 0.2678 M of H_2O. Figure 4.2 also shows that the hydrodynamic diameter of the water droplet in the W/O microemulsions decreases drastically from 16 to 10 nm with an increase in the butanol

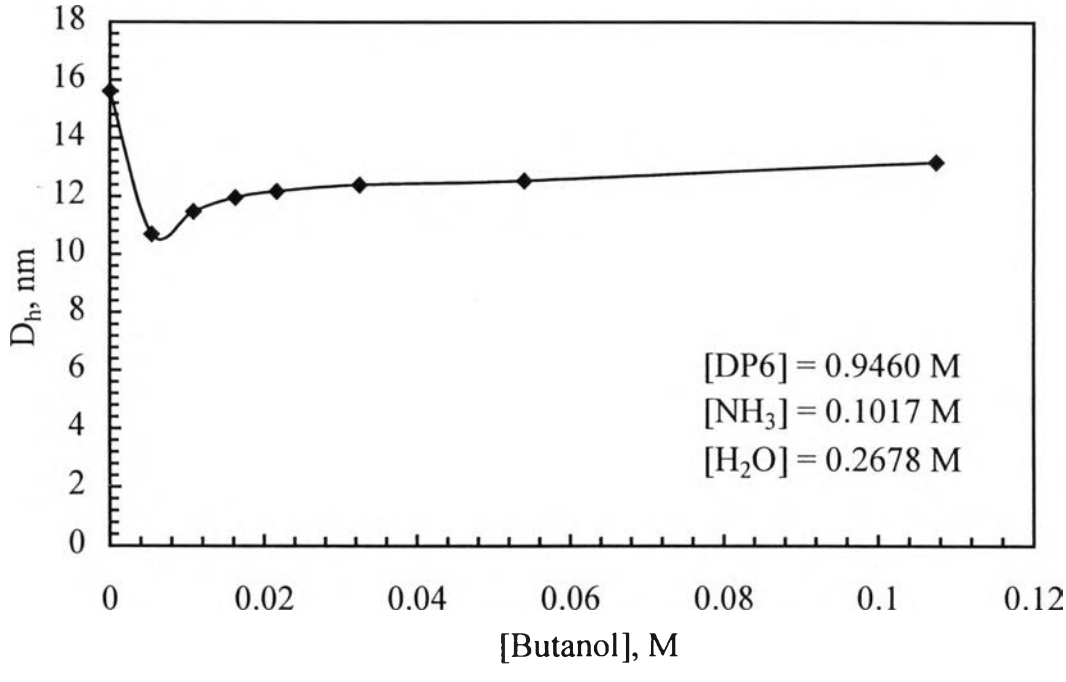

Figure 4.2 Effect of butanol concentration on hydrodynamic diameter of micelles in the W/O microemulsion system containing of DP6, heptane, and aqueous ammonia

concentration in the range of less than 0.006 M. Beyond this butanol concentration, the diameters of the micelles gradually increased and eventually level off constant approximately about 13 nm. The results indicate that addition of a small amount of butanol, the micelle droplet size decreases significantly as a result of formation of hydrogen bonding between ethoxyl (-OE) and hydroxyl (-OH) groups of DP6 and butanol molecules, respectively. The hydrocarbon tail groups of DP6 and butanol can also repel each other. This interaction can induce to increase not only the rigidity of interfacial layer of micelle, but also the curvature of microemulsion droplet (i.e., decrease in micelle diameter). The conformation of this action is illustrated in Figure 4.3. For the higher concentrations of butanol, the excessive butanol molecules, which have higher polarity than that of heptane, prefer to penetrate directly into aqueous core of microemulsion droplet as illustrated in Figure 4.3. This incident leads to slightly decrease the curvature of microemulsions but increase the dynamic exchange of aqueous component among microemulsion droplets.

4.2 Kinetics of Silica Particle Formation in W/O microemulsion

For kinetics studies, the rates of TBOS hydrolysis and silica particle growth were determined. The composition of the system studied is given in Table 4.1. Detail of the studies can be described as follows:

4.2.1 Rate of TBOS hydrolysis

The rate of TBOS hydrolysis was investigated by using Fourier transform infrared spectroscopy (FTIR). The FTIR spectra, illustrated in Figure 4.4 indicate the typical evolution of the TBOS hydrolysis in the W/O microemulsion solution. The FTIR spectra illustrate the vibrational stretching

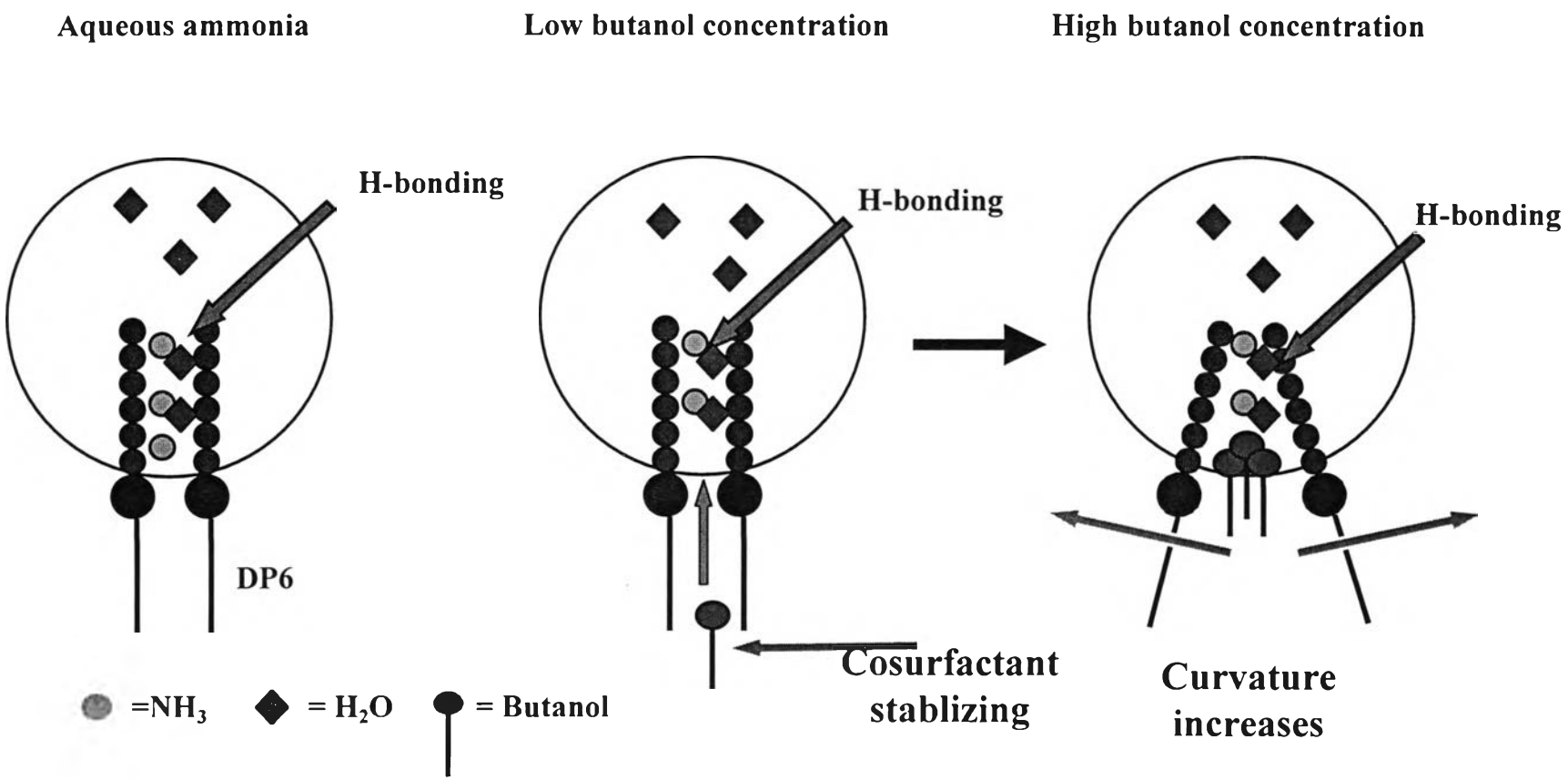

Figure 4.3 Schematics of butanol (co-surfactant) to stabilize water-oil interfacial layer

Table 4.1 Composition of the system studied

Components	Concentration (M)
DP6	0.9460
NH_3	0.1017
H_2O	0.2678
TBOS	0.0344

bands of TBOS's Si-O-C group located at both wavenumbers of 805 and 905 cm^{-1}. In comparison with the previous results, the Si-O-C spectra of TEOS and ethanol, were located at 795, 967, and 882 cm^{-1} (Chang and Fogler, 1996). These peaks decrease gradually with the reaction time and eventually disappear. The absorption spectra of TBOS (Si-O-C) can not only be located widely at different IR spectrum band, but also overlab the peak of butanol. In summary, the above FTIR can be calculated that TBOS is consumed in the microemulsions or the occurrence of TBOS hydrolysis reaction is in the microemulsions. Moreover, it indicates that $RSi(OH)_n$ has a fairly strong Si-OH vibrational band located in the range of 880-825 cm^{-1}. The hydrolyzed TBOS molecules condense into polymerized silica species immediately after they are produced.

The concentrations of TBOS at different reaction times were calculated from the heights' evolution of the 805 and 905 cm^{-1} peaks, respectively. As can be seen from Figure 4.5, the TBOS concentration depletes exponentially to zero. The results indicate that hydrolysis of TBOS in microemulsions media is first-order reaction only depends on TBOS concentration.

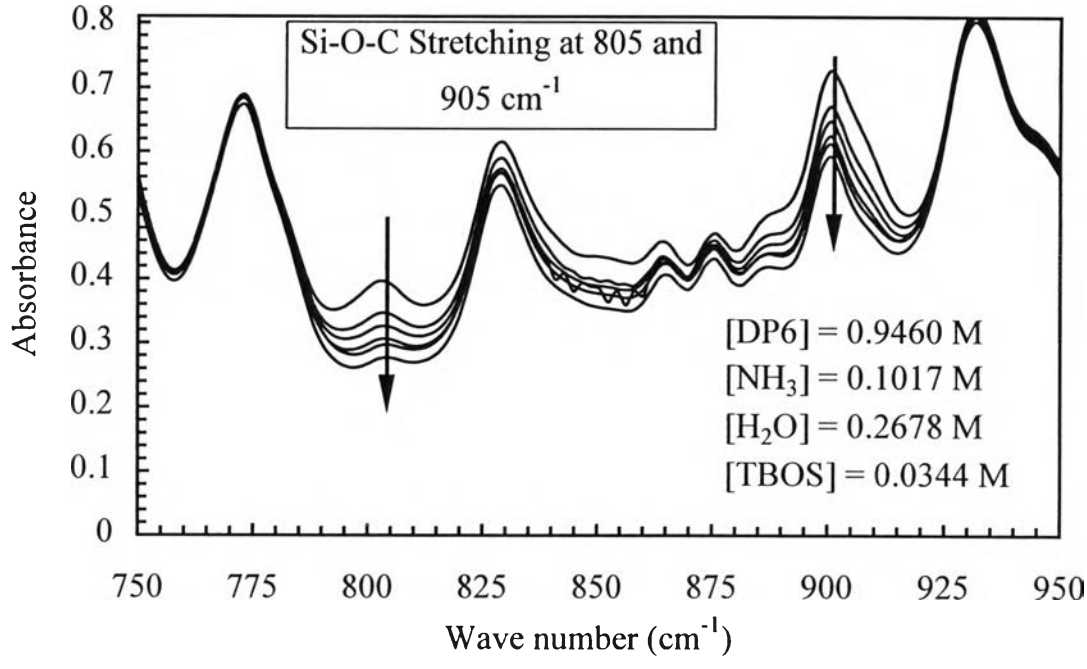

Figure 4.4 Time evolution of FTIR spectra during TBOS hydrolysis in W/O microemulsion system

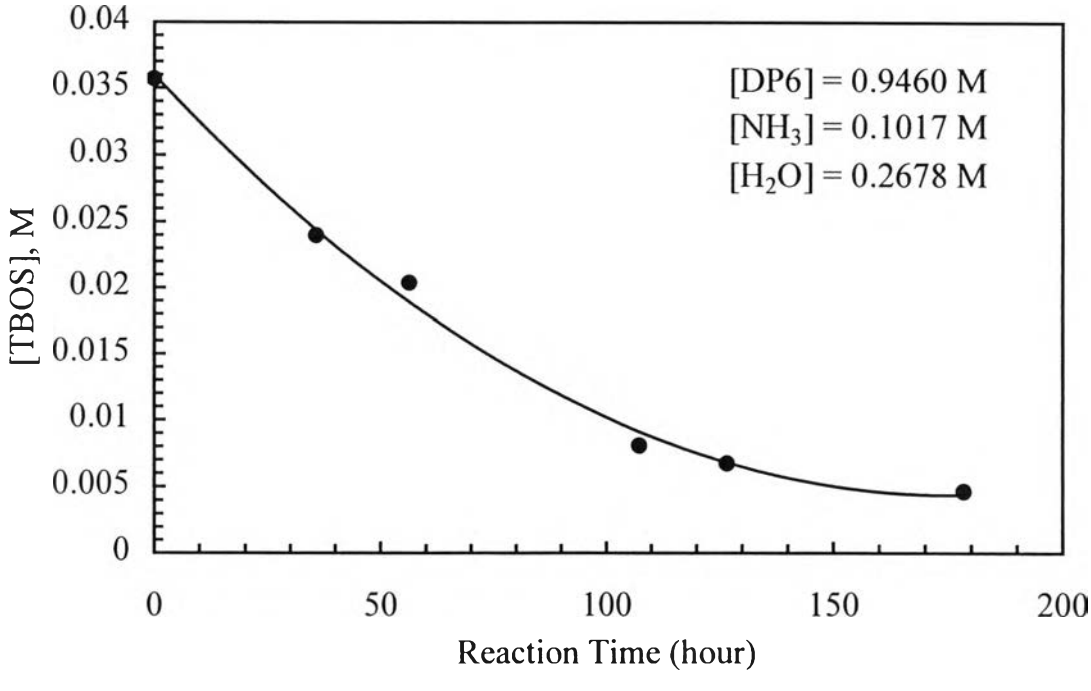

Figure 4.5 Concentration of TBOS during TBOS hydrolysis in W/O microemulsion system

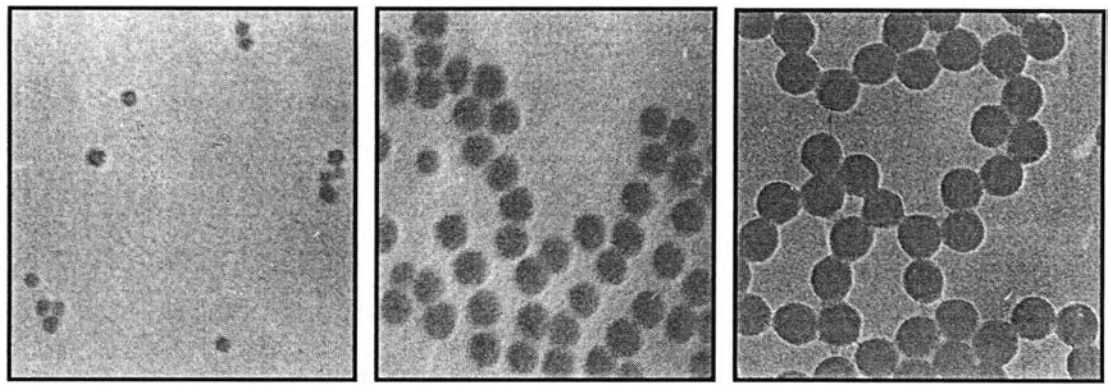

1.98 h **22.22 h** **113.93 h**

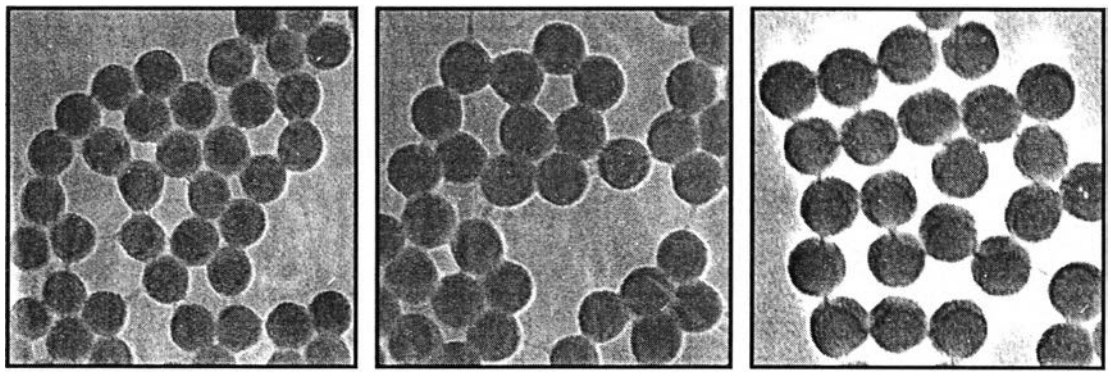

170.07 h **192.47 h** **229.07 h**

(—— = 50 nm)

Figure 4.6 TEM micrographs indicating the silica particle growth during TBOS hydrolysis

4.2.2 Time Evolution of Silica Particles

The rate of silica particle growth through TBOS hydrolysis in the nonionic microemulsions was studied by using a transmission electron microscopy. The evolution of silica particles is illustrated by the TEM micrographs taken at different time periods as shown in Figure 4.6. These pictures show those silica particles as forming mono-layers predominately

attach directly on the surface of carbon-coated copper grid during taking a picture. This can be deduced that silica particles well dispersed in the original solution. The spherical silica particles were revealed virtually by utilizing TEM micrographs, after the reaction went on for longer than 2 hours. The actual time of silica particle growth in the nucleation period was difficult to be measured with the current techniques. The monodispersed silica particles were illustrated with the enlarged micrographs. The appearing diameter of silica particles, can be measured by using View Capture Apparatus. TEM micrographs also verify that the shape of silica particle size distributions remains almost uniformly during the reaction. This result agrees very well with the study of Chang and Fogler (1996, 1997), which used another typical alkoxide reagent (TEOS) to study the growth of silica particle in different nonionic W/O microemulsions.

The size distribution of silica particles at different reaction times is shown in Figure 4.7. The size distribution in the initial stage is obviously wider than in the finally reaction period. The width of size distribution is approximately spanned less than 10 nm in the last period. The average diameter <D> and the normalized standard deviation $\sigma/<D>$ of these size distributions are presented in Figure 4.8. As can be seen from Figure 4.8, the silica particles grow quickly at the initial period of formation. After the reaction went on for about 10 days, the growth rate became slower and the final size was approximately 50 nm in 230 days. This value of the final size is significantly larger than the size of microemulsion droplets (about 4 times larger). The particle size distribution of silica particle can be attained from the values of $\sigma/<D>$. The normalized standard deviation gradually decreased from 10% at 1.98 hours to 2% at the end of reaction. The consistency of the size distribution appearance and the normalized standard deviation indicate the size increment (i.e., $dD/dt \sim D^0$) during the silica particle growth in W/O microemulsions. One issue of the kinetics of silica particle formation in W/O microemulsion is

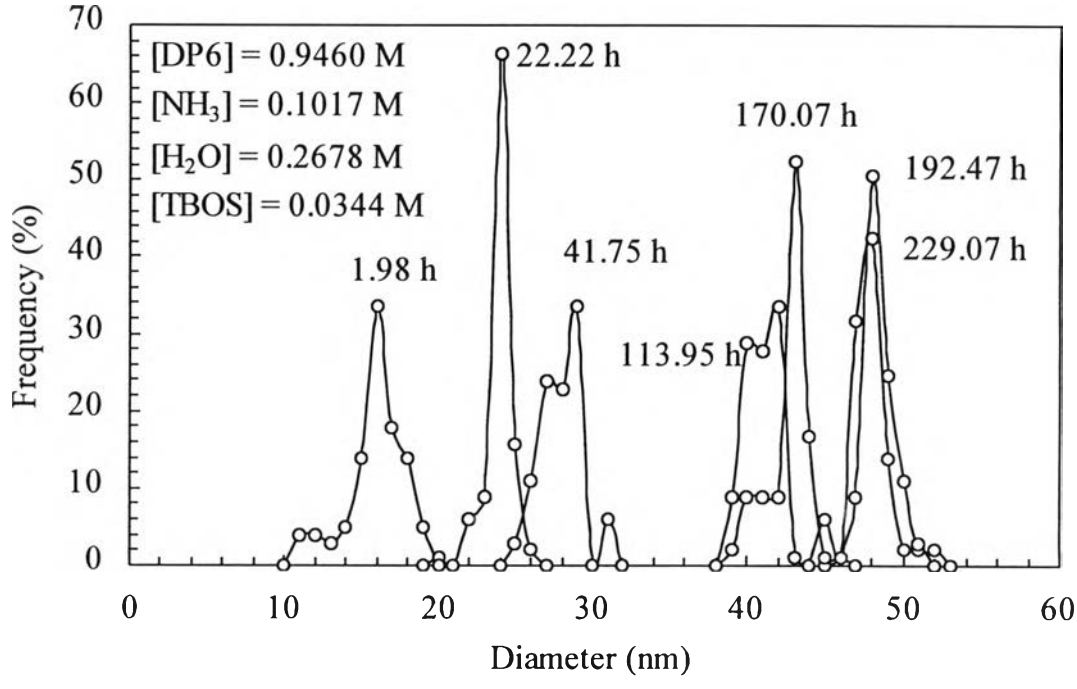

Figure 4.7 Size distribution of silica particle growth during TBOS hydrolysis in W/O microemulsion

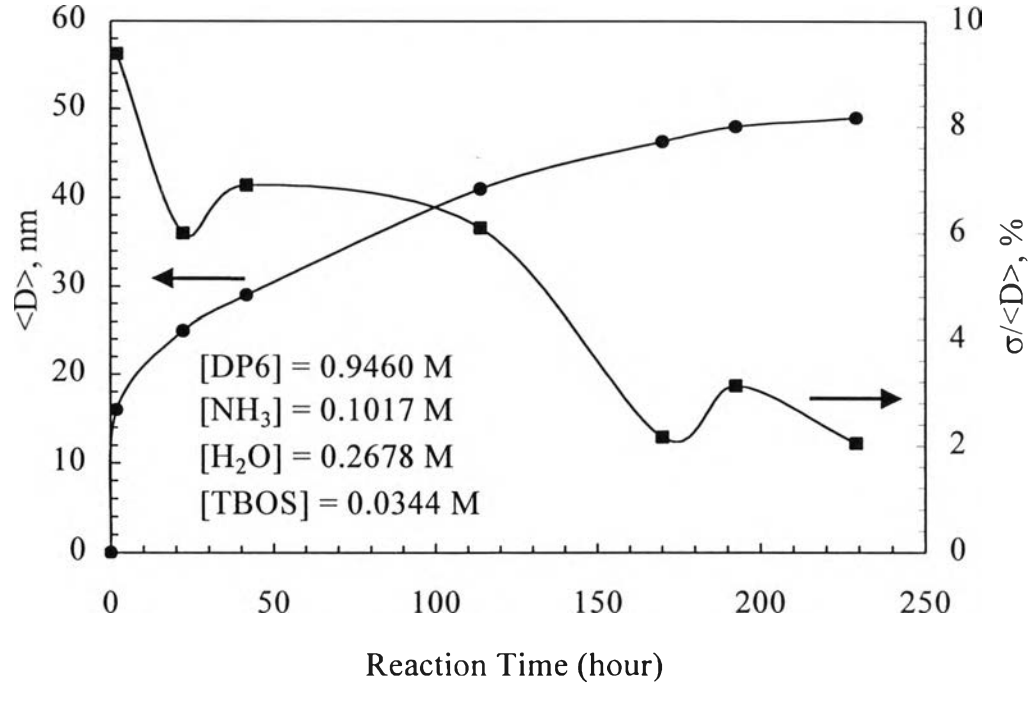

Figure 4.8 Average diameter, <D> and normalized standard deviation, σ/<D>, of silica particles during TBOS hydrolysis

offered in terms of the rate of silica particle growth by computing from the size increment. On the other hand, diffusion-controlled particle growth is characterized by a reduction of the standard deviation of particle sizes with the reaction time because the rate of particle size increment is conversely proportional to the diameter of particles (i.e. $dD/dt \sim D^{-1}$) (Dirksen and Ring, 1991).

The semi-logarithmic plot as illustrated in Figure 4.9, shows the linear depletion of TBOS concentration and evolution of particle size versus reaction time corresponding to equations (3.5) and (3.7), respectively. This straight line also describes both the kinetics of silica formation and TBOS hydrolysis. Therefore, the first four initial data points were used to compute the apparent rate constants for TBOS hydrolysis (k_h) and silica particle growth (k_c). These calculated values of k_h and k_c are 0.0082 h^{-1} and 0.0084 h^{-1} respectively. The closeness between these two calculated values of k_h and k_c

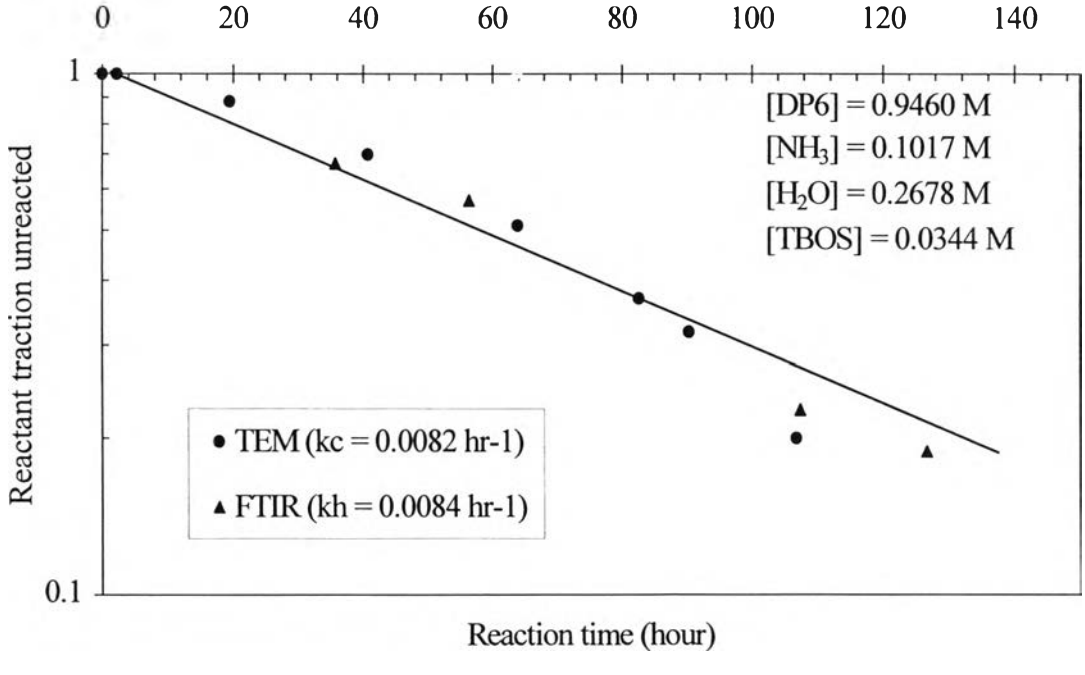

Figure 4.9 Comparison of the rate of TBOS hydrolysis and silica particle growth in W/O microemulsion

deduces that the growth of silica particles is controlled by the extremely slow rate of TBOS hydrolysis. Therefore, TBOS hydrolysis is the determining-step reaction for the silica particle formation in the W/O microemulsion media. The similar conclusions were also given in the previous studies (Chang and Fogler, 1996; Chang and Fogler 1997; and Arriagada and Osseo-Asare, 1995).

From the results of FTIR and TEM measurements, it indicates that the extremely slow hydrolysis rate of TBOS controls the growth of silica particles in the W/O microemulsion droplets. The hydrolysis of TBOS influences the shape and size distribution of silica particles formed. Due to the uniform distribution of TBOS in the external oil phase, the extremely slow TBOS hydrolysis occurs onto the surface of all microemulsion droplets at the same rate. Therefore, the concentration of hydrolyzed TBOS species is sufficiently low and insignificant concentration gradient set up around each growing silica particle. Consequently, the rate of hydrolyzed TBOS species condensing onto the silica particle surface is independent of the particle dimensions. The evolution of silica particle size distribution is controlled with the rate of TBOS reaction (Chang and Fogler, 1996).

TEM micrographs also suggest that, the hydrolyzed TBOS can form silica particle immediately after the particle nucleation. Since the size of silica particles is much larger than that of the microemulsion droplets, the silica particle number in W/O microemulsion solution can be calculated to be approximately 1.3×10^{18} (Appendix B). A decrease in particle size causes an increase in the number of silica particles formed (Arriagada, 1991). According to the slow hydrolysis rate of TBOS, the growing process of silica particle is significantly involved with the inter-micellar mass exchange. This process is coagulation of hydrolyzed monomeric and polymeric silica species among microemulsion droplets (Chang and Fogler, 1996; Chang and Fogler 1997; and Arriagada and Osseo-Asare, 1995).

From the results of TBOS hydrolysis, it indicates that the hydrocarbon chain length (-OR group) clearly influences the hydrolysis rate. In the fact of if the hydrocarbon length increases, the hydrolysis rate of alkoxide molecules will decrease. An increase in hydrocarbon atoms will reduce the partial charge distribution in the alkoxide molecule, leading to decrease the activity of M-OR bond (Livage, 1982). Chang and Fogler (1996) studied the kinetics of silica particle formation in W/O microemulsion system. They found that the apparent rate constant of TEOS hydrolysis (k_h) was 0.032 h^{-1} which is virtually 4 times greater than the value obtained in this study (k_h = 0.0084 h^{-1} for TBOS hydrolysis).

4.2.3 Controlling the Formation of Silica Particle in W/O Microemulsion Using Butanol

Although the recent work had studied the effects of alcohol types and their composition in the W/O microemulsion system, the results still could not be clearly explained (Esquena et al., 1997). In this experimental study, 1-butanol as a co-surfactant was applied to improve the interfacial property of W/O microemulsion droplets. The influence of butanol concentration on average size of silica particle <D> and normalized standard deviation $\sigma/<D>$ is shown in Figure 4.10. These measured values were obtained after the reaction was carried out for 10 days by using TEM micrograph and view capture apparatus. Under the presence of butanol at using low concentration, the average diameter of silica particle was gradually decreased when the butanol concentration was increased. The minimum value of the average diameter was reached virtually at 38 nm at 0.0161 M of butanol concentration. In this range of butanol concentration value of $\sigma/<D>$ decreased from 3 % to 1.5 %. When the butanol concentration exceeded 0.0161 M, the values of <D>, and $\sigma/<D>$ increased substantially with an increase in the butanol concentration. The final

size of silica particles formed after 10 days at different butanol concentration is illustrated by TEM micrographs in Figure 4.11. As can be seen from these photographs, the addition of 0.0161 M of butanol gives the narrowest size distribution when compared to 0 M and 0.1061 M which give the wider size distribution. These results show that the presence of small amount of butanol will increase the rigidity of interfacial layer by hydrogen bonding between OE and OH groups, leading to a small size of micelles (Esquena et al., 1997). Hence, the more rigidity or less fluid-like of interfacial layer causes to decrease the inter-micellar mass exchange. For a higher concentration of butanol as shown in Figure 4.2, more butanol molecules can penetrate into micelle layer and then slightly increase the curvature of microemulsion droplets. Due to this penetration of butanol molecules, it leads to increase the dynamic exchange of aqueous component between microemulsion droplets. Therefore, the size of silica particles can dramatically increase, since the interchanging of matter inside micelles cannot be avoided.

The hydrolysis rate constant (k_h) as shown in Figure 4.12 is changed with respects to the butanol concentration. It showed that the value of k_h decreased gradually when the concentration of butanol increased, because of the excessive amount of butanol mutated the equilibrium of reaction. The referred reactions are of the formation of silica particle from TBOS hydrolysis were described earlier in chapter 2. Usually, the hydrolyzed TBOS species have more presumable to polymerize with the silica particle formed than to create a new nuclei. Once, the hydrolysis rate constant decreases and is much slower than the rate of inter-micellar mass exchange which results in increasing of empty-core of microemulsion droplets. The hydrolyzed silica species have higher probability to form the nucleic silica particle in the empty aqueous core. Consequently, the size of resultant silica particle will span wider when using the higher concentration of butanol.

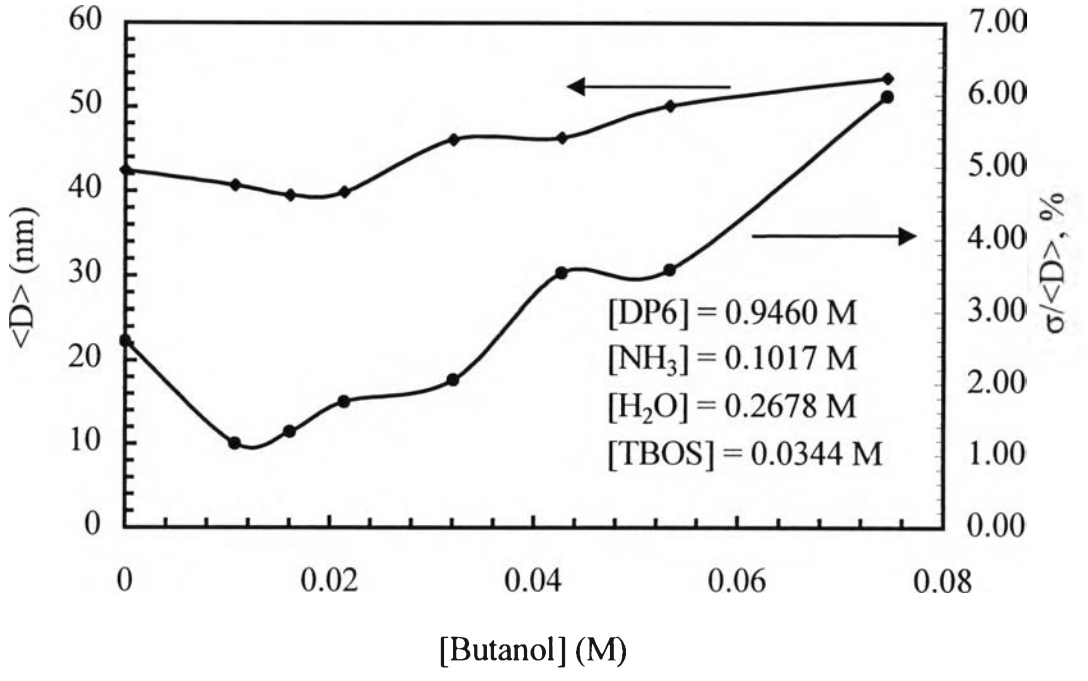

Figure 4.10 Effect of butanol concentration on <D> and σ/<D>

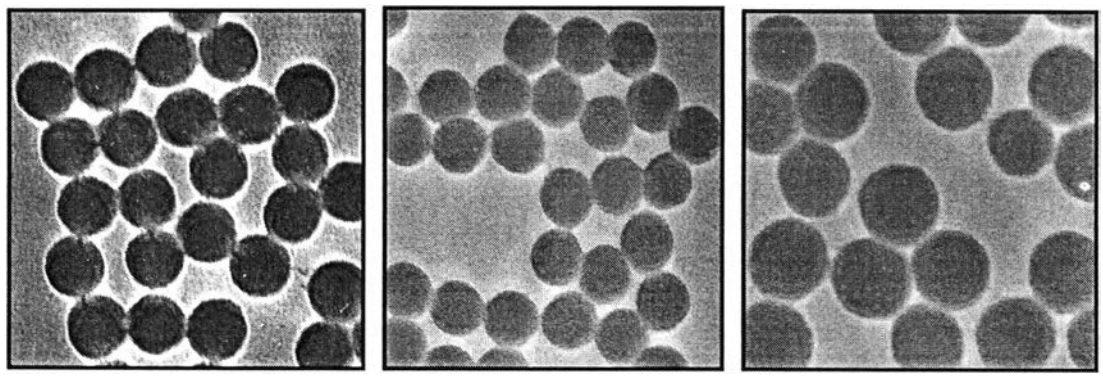

0 M **0.0161 M** **0.1061 M**

(——— = 50 nm)

Figure 4.11 TEM micrographs indicating the effect of butanol concentration on final period of silica particle size after 10 days reaction time

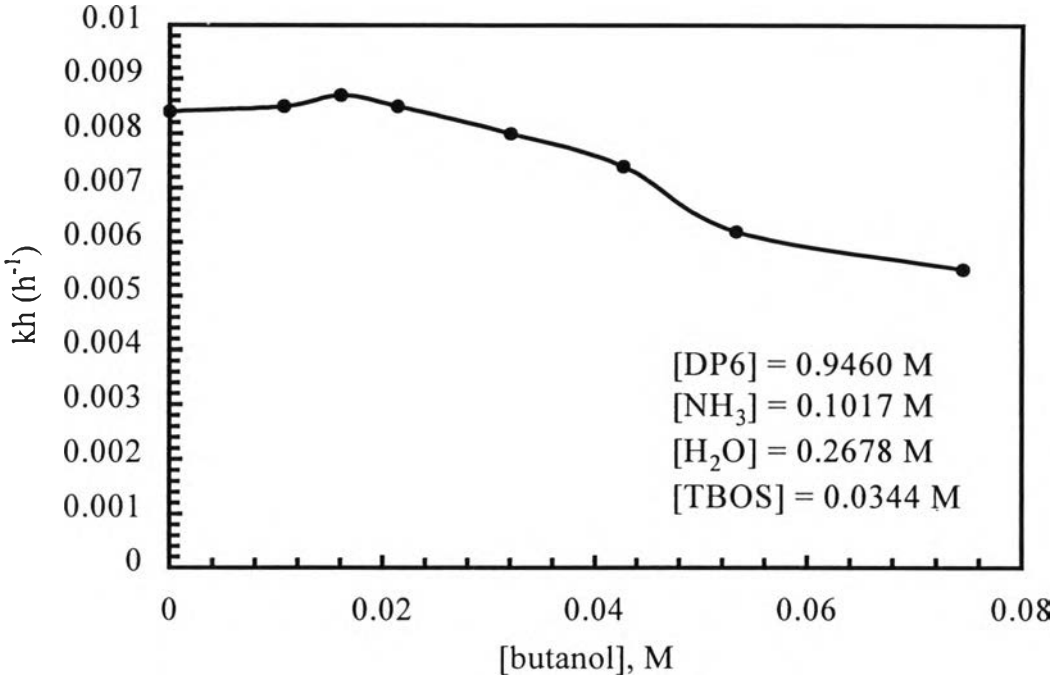

Figure 4.12 Effect of butanol concentration on the kinetic constant of TBOS hydrolysis